Available online at www.sciencedirect.com
SCIENCE DIRECT®
ELSEVIER
Optics Communications 235 (2004) 261–267
OPTICS COMMUNICATIONS
www.elsevier.com/locate/optcom

Bragg properties of efficient surface relief gratings in the resonance domain

M.A. Golub *, A.A. Friesem, L. Eisen

Department of Physics of Complex Systems, Weizmann Institute of Science, P.O. Box 26, Rehovot 76100, Israel

Received 30 December 2003; received in revised form 24 February 2004; accepted 24 February 2004

Abstract

Closed form analytical solutions of diffraction efficiency for transmission surface relief gratings in the resonance domain are presented. These are obtained by modeling the surface relief gratings with equivalent graded index gratings having Bragg properties, so as to allow for an optimum choice of grating parameters that would lead to high diffraction efficiencies. The calculated and experimental results reveal that the diffraction efficiency can be greater than 85% with optimized grating parameters within their certain strict limits.

PACS: 42.40.Lx.; 42.25.Fx.; 42.40.Eq.; 42.79.Dj

Keywords: Diffraction grating; Rigorous diffraction theory; Binary optics; Digital holography

Surface relief gratings in the resonance domain, where the grating period is comparable to that of the illumination wavelength, have a unique diffraction efficiency peak [1,2]. The physical nature of this peak is not yet understood completely [3,4]. In order to analyze such gratings, it is usually necessary to resort to extensive numerical methods of rigorous diffraction theory, presented for example in [1,2,5–8]. This is particularly so when optimizing the various grating parameters and trade-offs for surface relief gratings in the resonance domain in order to obtain the best diffraction efficiencies.

In this paper, we present a new approach for analyzing resonance domain surface relief gratings. It is based on ‘‘equivalent’’ sinusoidal graded index gratings model, and provides analytic, closed form solution for evaluating the performance of surface relief gratings with arbitrary groove shapes and diffraction efficiencies. Moreover, the model explains the unique diffraction efficiency peak and provides constraints on the grating parameters for which high diffraction efficiencies can be achieved.

We begin by considering a basic surface relief grating, recorded on a planar substrate, that is illuminated with a monochromatic oblique plane

* Corresponding author. Tel.: +972-8-9342032; fax: +972-8-9344109.
E-mail address: michael.golub@weizmann.ac.il (M.A. Golub).

0030-4018/$ - see front matter
doi:10.1016/j.optcom.2004.02.069

wave of wavelength λ at an incidence angular orientation of θ_{inc}. The period of this grating is Λ_x, and the grooves are slanted for obtaining high diffraction efficiency. The relevant parameters and geometry of one groove from such a grating are depicted on the Fig. 1. The refractive index of groove material is n_M, refractive index of upper layer n_i, maximum depth of grooves h_{max} measured normal to the plane substrate. The distribution of the refractive index n of the groove has the values of either n_i or n_M. Finally the normalized groove shape is defined by function $g(\chi)$, where the normalized coordinate χ ranges from 0 to 1, within a single grating groove, and $0 \leqslant g(\chi) \leqslant 1$.

In dealing with slanted grooves, we found it convenient to rotate the coordinate system by a slant angle φ_0, whose value must be optimized. In the rotated coordinate system the grooves are characterized by a normalized coordinate χ_ξ, a normalized "slanted groove shape" $g_\zeta(\chi_\xi)$, a slanted grating period $\Lambda_\xi = \Lambda_x \cos\varphi_0$ and a slanted maximum depth of groove $h_{max\,\zeta} = h_{max}/\cos\varphi_0$. Applying usual coordinate rotation equations, followed by simple algebraic manipulations, yields

$$g_\zeta(\chi_\xi) = g(\chi) \quad \text{and} \quad \chi_\xi = \chi - pg(\chi) \tag{1}$$

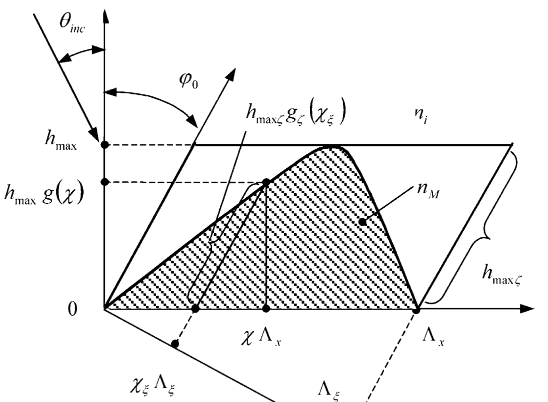

Fig. 1. Parameters and geometry of one groove in the surface relief grating before and after coordinate rotation at angle φ_0. Here θ_{inc} denotes the angle of incidence; n_M and n_i the refractive indices of the grating groove material and the upper layer; Λ_x, Λ_ξ the grating period, h_{max}, $h_{max\,\zeta}$ the maximum groove depths and $g(\chi)$ and $g_\zeta(\chi_\xi)$ the groove shapes before and after coordinate rotation.

with the "slant parameter" defined as $p = h_{max}\tan\varphi_0/\Lambda_x$.

We now develop the sinusoidal graded index model of the surface relief grating with slanted grooves. We begin by approximating n^2 with a two-dimensional complex Fourier series, as

$$n^2 = n_0^2 + \Delta n_M^2 \sum_j G_j \exp(\mathrm{i}2\pi j\chi_\xi), \tag{2}$$

where $\Delta n_M^2 = n_M^2 - n_i^2$, and a slant angle φ_0, which is incorporated in χ_ξ (see Eq. (1)), must be optimized. The essentially constant parameters n_0^2 and G_j can be determined by routine mathematical least square approximation, to yield

$$n_0^2 = \langle n^2 \rangle, \quad G_j = \left\langle \frac{n^2 - n_0^2}{\Delta n_M^2} \exp\left(-\mathrm{i}2\pi j\chi_\xi\right) \right\rangle, \tag{3}$$

where $\langle\,\rangle$ denotes averaging within a single grating groove, both in width and height. The mean-square refractive index n_0^2 in Eq. (3) is calculated by integration of function n^2 along the normal to the grating, to yield

$$n_0^2 = n_i^2 + \Delta n_M^2 \bar{g}, \quad \text{with} \quad \bar{g} = \int_0^1 g(\chi)\,\mathrm{d}\chi. \tag{4}$$

The value of the dominant first harmonic term coefficient G_1 is found by integration of piecewise constant function n^2 along the slant angle φ_0 direction, to yield

$$G_1 = \int_0^1 g_\zeta(\chi_\xi) \exp\left(-\mathrm{i}2\pi\chi_\xi\right) \mathrm{d}\chi_\xi. \tag{5}$$

We now introduce a refractive index modulation term Δn, which is derived by comparing Eq. (2) to that obtained for sinusoidal graded index gratings [9], as

$$\Delta n = \frac{\Delta n_M^2}{n_0} |G_1|. \tag{6}$$

The refractive index modulation Δn in Eq. (6) depends on the difference between n_M and n_i, the groove profile shape and slant parameter p. In order to determine the "equivalent" graded index grating, which best characterizes the surface relief grating, it is necessary to properly choose the slant angle φ_0 or alternatively the slant parameter p. Denoting p_s as that value of p at which the maximum values of Δn and $|G_1|$, occur, i.e. $\Delta n = \Delta n_s$ and $|G_1| = G_{1s}$, we find that the optimum slant angle φ_s can be determined from

$$\tan\varphi_s = \frac{\Lambda_x}{h_{\max}} p_s. \tag{7}$$

Eq. (7) leads to the dominant "equivalent" graded index grating that corresponds to a specific surface relief grating. Such an equivalent grating thus simulates most accurately the surface relief grating in terms of the highest possible value of Δn, i.e. $\Delta n = \Delta n_s$. Specifically Eqs. (4) and (5) together with Eqs. (1) and (7) essentially denote the most important relations between the surface relief grating and its sinusoidal graded index grating model. Together they simplify the complicated calculation of diffraction efficiencies for surface relief gratings in the resonance domain to those of relatively simple calculation for sinusoidal graded index model gratings.

Besides the dominant equivalent graded index grating with p_s and φ_s, there are additional gratings with p and φ_0 that degrade the overall efficiency. In general, it is necessary to consider only those additional gratings, which have relatively high Δn. In particular, only those with $|\Delta n/\Delta n_s| \geqslant \delta_{\mathrm{low}}$, where δ_{low} is a fixed small threshold value. In other words, we consider only additional gratings with p between boundaries p^-_{low} and p^+_{low} defined by equations $p^\pm_{\mathrm{low}} = p_s \pm \Delta p_{\mathrm{low}}$ and $|\Delta n/\Delta n_s||_{p=p^\pm_{\mathrm{low}}} = \delta_{\mathrm{low}}$.

As a representative example we investigate the surface relief grating of slanted sinusoidal groove shape characterized by a relative groove peak position q_c, with $0 \leqslant q_c \leqslant 1$ within the groove. In accordance to Eqs. (4) and (5), $\bar{g} = 0.5$, $p_s = q_c - 0.5$ and the parameters G_1 and n_0 are

$$|G_1| = \frac{1}{2}\left|\frac{J_1[\pi(p-p_s)]}{\pi(p-p_s)}\right|, \qquad n_0 = \sqrt{(n_M^2 + n_i^2)/2}. \tag{8}$$

Eq. (8) indicates that G_1, and consequently Δn of Eq. (6), have maximum values $G_{1s} = 0.25$ and $\Delta n_s = 0.25\Delta n_M^2/n_0$ at $p = p_s$, and side lobes. In this example, $\Delta p_{\mathrm{low}} = 1.052$, in accordance with a threshold value δ_{low} which was chosen as the ratio of the first side lobe peak to the maximum value.

For an arbitrary slant parameter p, the jth order Bragg conditions [9] can be written as

$$s_j^2 + c_j^2 = 1, \tag{9}$$

where, in our notations, s_j and c_j are

$$s_j = \frac{n_i}{n_0}\sin\theta_{\mathrm{inc}} - j\frac{\lambda}{n_0\Lambda_x},$$
$$c_j = \sqrt{1 - s_0^2} - j\frac{\lambda}{n_0 h_{\max}} p. \tag{10}$$

Solving Eqs. (9) and (10) leads to the Bragg incidence angles $\theta_{\mathrm{inc},j}$ at wavelength λ for the resonance domain surface relief grating, as

$$n_i \sin\theta_{\mathrm{inc},j} = \frac{j\lambda}{2\Lambda_x} - \frac{\Lambda_x p}{h_{\max}}\left[\frac{n_0^2}{1 + (\Lambda_x p/h_{\max})^2} - \left(\frac{j\lambda}{2\Lambda_x}\right)^2\right]^{1/2}. \tag{11}$$

The dominant +1st Bragg incidence angle $\theta_{\mathrm{inc},1}|_{p=p_s}$ of the surface relief grating can be obtained from Eq. (11) with $j = +1$ and $p = p_s$.

Using the equivalent grating model, the calculation of the +1st order diffraction efficiency η_1 for highly efficient surface relief gratings, is now reduced to exploiting the relatively simple closed form analytic relation from the theory of the sinusoidal graded index grating [9], of

$$\eta_1 = \sin^2\left(\sqrt{\nu_1^2 + \xi_1^2}\right)\left[1 + (\xi_1/\nu_1)^2\right]^{-1}. \tag{12}$$

The parameters ν_1 and ξ_1 are now specific for surface relief gratings, where ξ_1 for either TE or TM polarization is

$$\xi_1 = \frac{\pi h_{\max} n_0}{2c_1\lambda}\left[1 - s_1^2 - c_1^2\right] \tag{13}$$

and ν_1 is different for TE and TM polarizations, as

$$\nu_{1TE} = \frac{\pi h_{\max}}{\lambda\sqrt{c_0 c_1}} \frac{(n_M^2 - n_i^2)}{n_0} G_{1s} \tag{14}$$

and

$$\nu_{1\mathrm{TM}} = \nu_{1\mathrm{TE}}\left\{1 - \frac{1}{2}\left(\frac{\lambda}{n_0\Lambda_x}\right)^2\left[1 + \left(\frac{\lambda p_s}{h_{\max}}\right)^2\right]\right\} \tag{15}$$

with c_0, c_1, s_1 defined by Eq. (10) when $p = p_s$.

Using Eqs. (5) and (12)–(15), we can draw several important conclusions. Letting $\xi_1 = 0$ in

Eq. (12), is equivalent to satisfying the Bragg condition whereby η_1 becomes the Bragg efficiency $\eta_{\rm Bragg}$. Then for a specific value of $\eta_{\rm Bragg}$, the depth of groove $h_{\max}$ can be found as a function of grating period Λ_x. Another interesting conclusion derived from Eqs. (5) and (12)–(15) is that in our treatment the Bragg efficiency of surface relief transmission gratings in the resonance domain is fully determined by the first Fourier coefficient of normalized slanted groove shapes calculated in the dominant slant direction of equivalent graded index grating. Still another conclusion is that surface relief gratings with different groove shapes will have the same Bragg efficiency when the Fourier coefficients of the normalized slanted groove shapes are equal. This conclusion is in agreement with the empirical criterion of "equivalence rule" for surface relief gratings [1,10].

Any small deviation of the incidence angle $\theta_{\rm inc}$ from the Bragg incidence angle $\theta_{{\rm inc},1}|_{p=p_s}$ or deviation of the illumination wavelength from the Bragg wavelength at given Bragg angle, corresponds to varying the parameter ξ_1, i.e. $\xi_1 \neq 0$. This leads to a small relative reduction of the Bragg efficiency to $\eta_{\rm mis}\eta_{\rm Bragg}$, where the reduction factor is $\eta_{\rm mis}$ ($0.8 \gtrsim \eta_{\rm mis} \leqslant 1$). From Eq. (12) we can readily determine analytical expression for the angular $\Delta\theta_{{\rm inc},1}$ and spectral $\Delta\lambda_1$ selectivities for highly efficient surface relief gratings as the bandwidth of diffraction efficiency response corresponding to the threshold level $\eta_{\rm mis}\eta_{\rm Bragg}$.

In order to determine the constraints of our approach, we must include in the analysis the degrading influence of additional gratings with slant parameter p between boundaries $p^-_{\rm low}$ and $p^+_{\rm low}$. In accordance to Eq. (11), when $j=-1$, some of the light from each additional graded index grating, in particular for increasing values of Λ_x/λ, will be diffracted into the -1st order instead of the +1st order. To ensure that this undesirable diffracted light is minimal, the Bragg incidence angle $\theta^-_{\rm inc,low} = \theta_{{\rm inc},-1}|_{p=p^-_{\rm low}}$ of the "worst case" additional grating with $p = p^-_{\rm low}$ must be sufficiently different from the +1st Bragg incidence angle $\theta_{{\rm inc},1}|_{p=p_s}$ of the dominant equivalent grating. In such a case the diffraction efficiency η_1 at the boundary $\theta^-_{\rm inc,low}$ should be lower than $\eta_{\rm mis}\eta_{\rm Bragg}$ and, in the worst case, becomes

$$\eta_1\Big|_{\theta_{\rm inc}=\theta^-_{\rm inc,low}} = \eta_{\rm mis}\eta_{\rm Bragg}. \qquad (16)$$

Eq. (16) gives main restriction of applicability of our model. For a given groove depth $h_{\max}$, the ratio Λ_x/λ is constrained to be smaller than an upper bound value $\Lambda_{x,{\rm up}}/\lambda$. This upper bound value is found by substituting Eq. (12) with $j=+1$ and $p=p_s$ and also Eq. (11) with $j=-1$ and $p=p^-_{\rm low}$ into Eq. (16).

To verify our model, we performed numerical calculations using rigorous coupled wave analysis [1,5,6]. We found that the results with our analytic model are in agreement with the numerical calculations, especially those for deep gratings [11] as depicted by thin and thick curves in Fig. 2. For example, for symmetrical sinusoidal gratings with $\lambda/\Lambda_x = 1.414$, $h_{\max}/\Lambda_x = 1.9$ and $n_M = 1.66$, the agreement for diffraction efficiency values is within 3% over the incidence angles ranging from 34° to 54°, with the Bragg incidence angle of 45°. This is shown in Fig. 3.

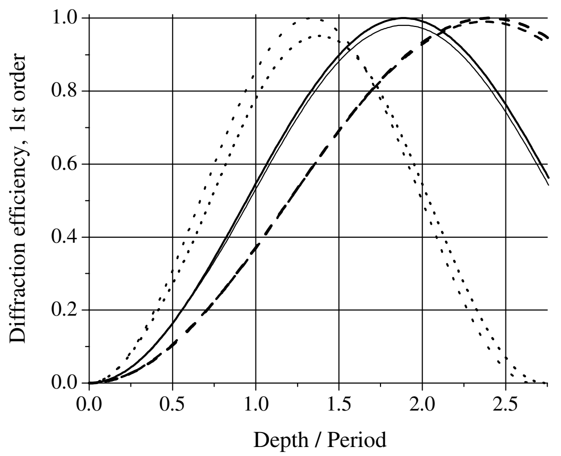

Fig. 2. The diffraction efficiency of the +1st order as a function of groove depth to period ratio $h_{\max}/\Lambda_x$, for symmetrical sinusoidal surface relief gratings. The Bragg incidence angle was 45°, ratio of readout illumination wavelength to the period $\lambda/\Lambda_x = 1.414$, refractive index of grooves $n_M = 1.50$, 1.66 and 2.0, and TE polarization. The thick-line curves are analytically calculated within the equivalent grating model of this paper, whereas the thin-line curves are numerically calculated by the rigorous coupled wave theory [11]. Analytical: - - - $n_M = 1.50$, – $n_M = 1.66$, ··· $n_M = 2.0$. Numerical: - - - $n_M = 1.50$, – $n_M = 1.66$, ··· $n_M = 2.0$.

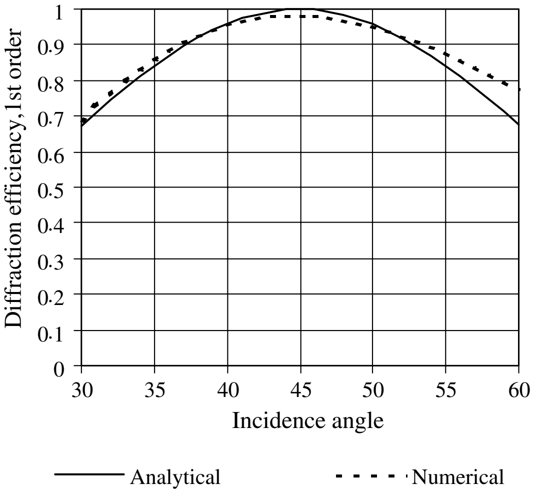

Fig. 3. The diffraction efficiency of the +1st order as a function of incidence angle, for symmetrical sinusoidal surface relief gratings. Ratio of groove depth to period $h_{\max}/\Lambda_x = 1.9$, ratio of readout illumination wavelength to the period $\lambda/\Lambda_x = 1.414$, refractive index of grooves $n_M = 1.66$, and TE polarization. Solid-line curve is analytically calculated within the equivalent grating model of this paper, dotted-line curve is numerically calculated within the rigorous coupled wave analysis.

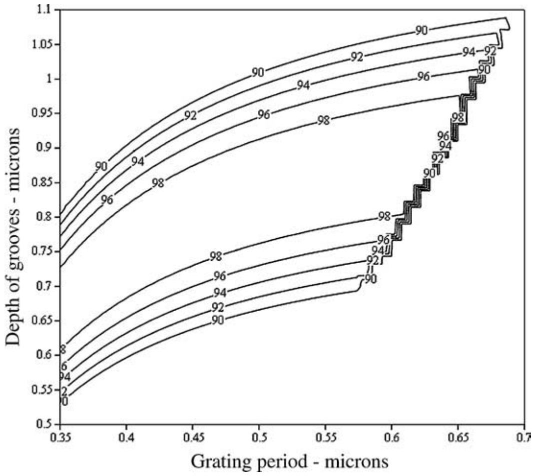

Fig. 4. Depth of grooves as a function of grating period and their limits for different Bragg diffraction efficiencies for sinusoidal surface relief gratings with slanted grooves shape. Slant angle $\varphi_s = 17°$, refractive index of groove material $n_M = 1.63992$ at the illumination wavelength $\lambda = 0.6328$ μm, and TE polarization.

To determine the relationship between the depth of grooves, the grating period and the diffraction efficiency within the bounds of our model, we considered a surface relief grating with slanted sinusoidal grooves shape and coefficient G_1 defined by Eq. (8). Incorporating $\Delta p_{\text{low}} = 1.052$ into Eq. (16), and using Eqs. (12)–(15) and (8), we calculated the depth of grooves as a closed form analytical function of the grating period at different Bragg diffraction efficiencies and found the limit of operation for such surface relief gratings, when the incident illumination wavelength is $\lambda = 0.6328$ μm and slant angle $\varphi_s = 17°$. The results for TE illumination are presented in Fig. 4. As shown, there are two ranges, where for a specific grating period, two different groove depths would result in the same diffraction efficiency. Also shown, at the right side border of the graph, is an upper bound $\Lambda_{x,\text{up}}$ that the grating period cannot exceed at a certain Bragg diffraction efficiency and groove depth. This important bound indicates that Bragg efficiency for surface relief gratings can be achieved only by satisfying both the Bragg condition and the bound $\Lambda_{x,\text{up}}$ determined from Eq. (16).

To experimentally verify our approach, we holographically recorded nearly sinusoidal surface relief gratings with slanted grooves shape, and measured their diffraction efficiency as a function of incident beam angular orientation. The gratings were obtained by recording the interference pattern of two plane waves that were derived from an Argon laser of wavelength $\lambda = 0.363$ μm. The recording material was Shipley 1813 photoresist with $n_M = 1.6399$ at the readout wavelength of $\lambda = 0.6328$ μm. The angular orientations of the recording plane waves and exposure levels were chosen to obtain a desired slant angle $\varphi_s = 17°$, grating period $\Lambda_x = 0.47$ μm, and groove depth $h_{\max} = 0.63$ μm. Fig. 5 shows a magnified scanning electron microscope photograph of a cross-sectional portion of this grating having a groove shape with slightly hard clipped planar upper part, but substantially sinusoidal lower part. Using the experimentally measured grooves profile shown in Fig. 5, we numerically estimated coefficient G_1 as function of slant parameter p and found that the actual slant angle of the equivalent grating is $\varphi_s = 17°$, as desired.

The experimental arrangement for measuring the diffraction efficiency of the gratings is sche-

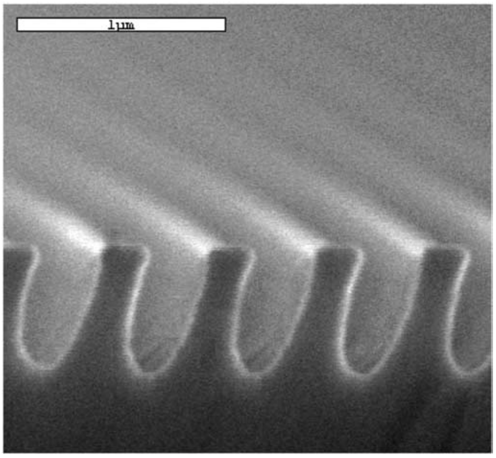

Fig. 5. Scanning electron microscope photograph depicting a magnified part of holographically recorded surface relief grating. Period $\Lambda_x = 0.47$ μm, groove depth $h_{\max} = 0.63$ μm and slant angle $\varphi_s = 17°$.

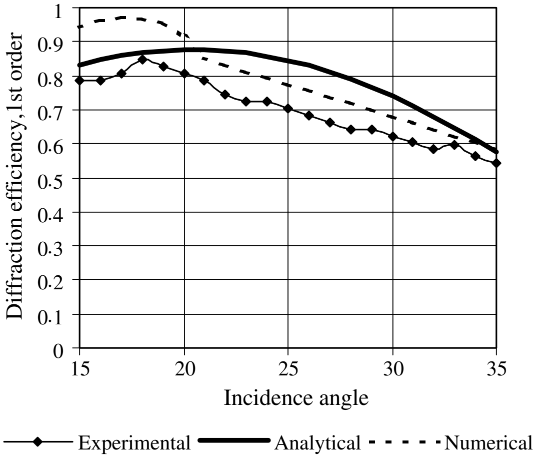

Fig. 7. The diffraction efficiency of the +1st order as a function of incidence angle for sinusoidal surface relief gratings with slanted grooves shape. Period $\Lambda_x = 0.47$ μm, groove depth $h_{\max} = 0.63$ μm and slant angle $\varphi_s = 17°$, readout illumination wavelength $\lambda = 0.6328$ μm, and TE polarization. Solid-line curve is analytically calculated within the equivalent grating model of this paper, dashed-line curve is numerically calculated within the rigorous coupled wave theory.

matically shown in Fig. 6. It is comprised of a He–Ne laser L with $\lambda = 0.6328$ μm, a grating G recorded in a photoresist layer which was deposited on a plane glass substrate, a prism P, a rotation stage S and a detector D. In order to measure the +1st diffraction order, which normally would be trapped by total internal reflection inside the glass substrate, we attached the substrate to the prism with index matching liquid. The prism and grating were placed on the rotation stage, so as to allow variation of incidence angles from 15° to 35° with 1° steps.

The results of the diffraction efficiency measurements, namely the power of +1st diffraction order over the incident power (after accounting for Fresnel reflections on the prism facets), as a function of incidence angle for TE illumination are presented in Fig. 7. Also included are the calculated results obtained both by the analytical calculations of our equivalent grating model and by numerical calculations of the rigorous coupled wave analysis. The analytically calculated maximum diffraction efficiency $\eta_{\mathrm{Bragg}} = 87.5\%$ occurs at a nonzero Bragg incidence angle $\theta_{\mathrm{inc},1} = 19.5°$. The Bragg angular selectivity is $\Delta\theta_{\mathrm{inc},1} = 15°$ and spectral selectivity $\Delta\lambda_1 = 0.2$ μm at a threshold level $\eta_{\mathrm{mis}} = 0.9$. As evident, the calculated and experimental results are in good agreement.

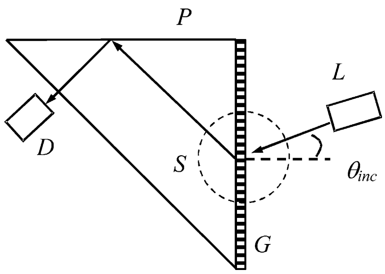

Fig. 6. Schematic experimental arrangement for measuring the grating efficiency. Here L denotes He–Ne laser with wavelength $\lambda = 0.6328$ μm, G – grating, D – power meter, P – prism, and S – a rotating stage.

In this paper, we developed and experimentally verified an equivalent graded index grating model explaining the Bragg behavior of resonance domain surface relief gratings and providing analytic solutions that can aid in grating design and optimization. Our results reveal that in order to achieve high diffraction efficiency for surface relief gratings certain constraints must be imposed, in addition to the Bragg conditions. These constrains define an upper bound for the grating period at given groove depths.

References

[1] E. Popov, E.G. Loewen, Diffraction Gratings and Applications, Marcel Dekker, Inc., New York, 1997.

[2] J. Turunen, M. Kuittinen, F. Wyrowski, in: E. Wolf (Ed.), Progress in Optics v.XL, Elsevier Science B.V., 2000, pp. 343–388.

[3] H.J. Gerritsen, D.K. Thornton, S.R. Bolton, Appl. Opt. 30 (1991) 807.

[4] T. Shiono, T. Hamamoto, K. Takahara, Appl. Opt. 41 (2002) 2390.

[5] M.G. Moharam, T.K. Gaylord, J. Opt. Soc. Am. 72 (1982) 1385.

[6] S. Peng, G.M. Morris, J. Opt. Soc. Am. A 12 (1995) 1087.

[7] L. Li, J. Chandezon, G. Granet, J.-P. Plumey, Appl. Opt. 38 (1999) 304.

[8] J.M. Miller, N. Beaucoudrey, P. Chavel, J. Turunen, E. Cambril, Appl. Opt. 36 (1997) 5717.

[9] H. Kogelnik, Bell Syst. Tech. J. 48 (1969) 2909.

[10] M. Breidne, D. Maystre, Appl. Opt. 19 (1980) 1812.

[11] K. Yokomori, Appl. Opt. 23 (1984) 2303.